Title

Cross-Tissue Single-Nucleus RNA Sequencing Discovers Tissue-Resident Adipocytes Involved in Propanoate Metabolism in the Human Heart.

Journal

Arteriosclerosis, Thrombosis, and Vascular Biology, 43(10)

Authors

Das, Sankha
Kar, Asha
Rajkumar, Sandhya
et al.

Publication Date

2023-10-01

DOI

10.1161/ATVBAHA.123.319358

Peer reviewed

HHS Public Access

Author manuscript

Arterioscler Thromb Vasc Biol. Author manuscript; available in PMC 2024 October 01.

Published in final edited form as:

Arterioscler Thromb Vasc Biol. 2023 October ; 43(10): 1788–1804. doi:10.1161/ATVBAHA.123.319358.

Cross-tissue single nucleus RNA-sequencing discovers tissue-resident adipocytes involved in propanoate metabolism in the human heart

Sankha Subhra Das[1], **Asha Kar**[1], **Sandhya Rajkumar**[1], **Seung Hyuk T. Lee**[1], **Marcus Alvarez**[1], **Kirsi H Pietiläinen**[2,3], **Päivi Pajukanta**[1,4,5,*]

[1]Department of Human Genetics, David Geffen School of Medicine at UCLA, Los Angeles, USA.

[2]Obesity Research Unit, Research Program for Clinical and Molecular Metabolism, Faculty of Medicine, University of Helsinki, Helsinki, Finland.

[3]HealthyWeightHub, Abdominal Center, Helsinki University Hospital and University of Helsinki, Helsinki, Finland.

[4]Bioinformatics Interdepartmental Program, UCLA, Los Angeles, USA.

[5]Institute for Precision Health, David Geffen School of Medicine at UCLA, Los Angeles, USA.

Abstract

Background: Adipocytes are crucial regulators of cardiovascular health. However, not much is known about gene expression profiles of adipocytes residing in non-fat cardiovascular tissues, their genetic regulation and contribution to coronary artery disease (CAD). Here, we investigated for the first time whether and how the gene expression profiles of adipocytes in the subcutaneous adipose tissue differ from adipocytes residing in the heart.

Methods: We used single-nucleus RNA-sequencing datasets of subcutaneous adipose tissue and heart, and performed in-depth analysis of tissue-resident adipocytes and their cell-cell interactions.

Results: We first discovered tissue-specific features of tissue-resident adipocytes, identified functional pathways involved in their tissue specificity, and found genes with cell-type-specific expression enrichment in tissue-resident adipocytes. By following up these results, we discovered the propanoate metabolism pathway as a novel distinct characteristic of the heart-resident adipocytes, and found a significant enrichment of CAD GWAS risk variants among the right atrium -specific adipocyte marker genes. Our cell-cell communication analysis identified 22 specific heart adipocyte-associated ligand-receptor pairs and signaling pathways, including THBS and EPHA, further supporting the distinct tissue-resident role of heart adipocytes. Our results also suggest chamber level coordination of heart adipocyte expression profiles as we observed a consistently larger number of adipocyte-associated ligand-receptor interactions and functional pathways in the atriums than ventricles.

[*]Correspondence: Päivi Pajukanta, MD, PhD, Professor of Human Genetics, David Geffen School of Medicine at UCLA, University of California, Los Angeles (UCLA), Gonda Center, Room 6357B, 695 Charles E. Young Drive South, Los Angeles, California 90095-7088, USA, ppajukanta@mednet.ucla.edu.

Disclosures

None.

Conclusions: Overall, we introduce a new function and genetic link to CAD for the previously unexplored heart-resident adipocytes.

Graphical Abstract

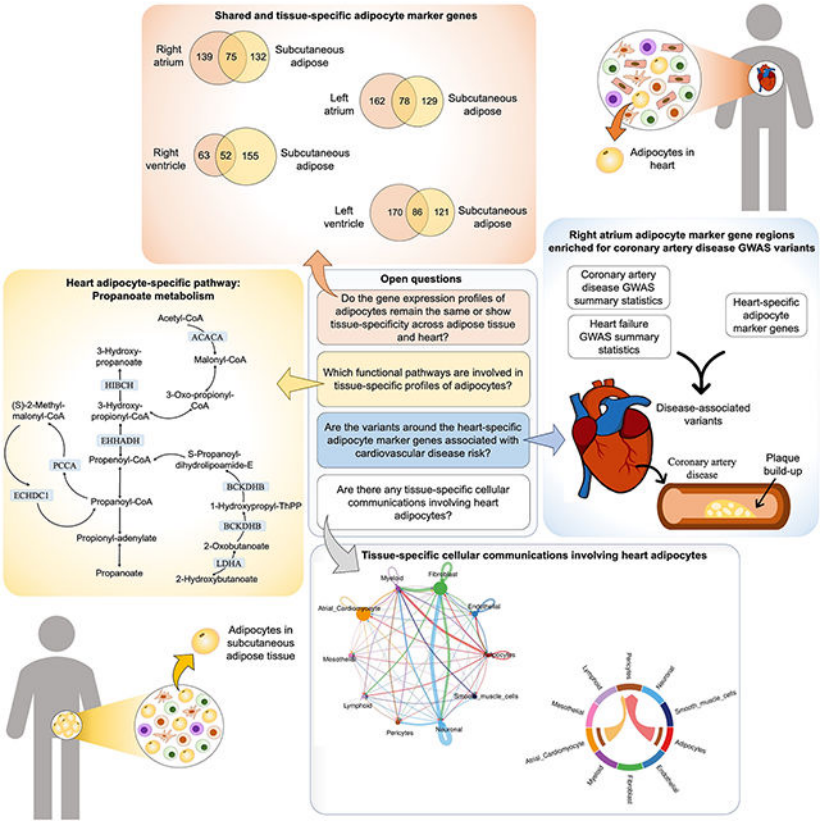

Keywords

adipocytes; heart; subcutaneous adipose tissue; propanoate metabolism; single nucleus RNA-sequencing

Introduction

Each human cell-type shows unique characteristics in its tissue environment. These tissue-specific properties of cell-types are regulated by genetic, epigenetic, and environmental factors that make cell-types distinct, depending on the tissue they reside[1]. Alterations in gene regulatory mechanisms affect the cell-type characteristics and contribute to a variety of complex diseases[2]. Therefore, understanding the molecular mechanisms of complex diseases needs extensive cell-type level investigation of heterogeneous tissues.

Adipocytes, the vital players of metabolic regulation, originate from mesenchymal stem cells (MSCs) through two sequential phases. The first phase involves the commitment of MSCs to preadipocytes and the second phase the differentiation from preadipocytes to mature adipocytes[3]. Adipocytes have a critical role in energy homeostasis. In response to energy status, adipocytes are able to change in number and/or size and maintain whole-body

energy balance[4]. However, the unhealthy expansion of adipocytes (i.e., hypertrophy) in obesity may contribute to the dysregulation of adipocyte-derived cytokines and metabolites, ultimately leading to complex cardiovascular diseases (CVDs)[5].

Although subcutaneous and visceral adipose tissue are the predominant fat depots of adipocytes, they can also be observed in other tissues, including the heart chambers i.e., left atrium (LA), left ventricle (LV), right atrium (RA), and right ventricle (RV)[6]. Previous studies have also reported that the epicardial fat, located between the visceral pericardium and myocardium, constitutes a significant proportion (~20%) of the total human heart mass[7]. Adipocytes in the human heart are involved in energy homeostasis and have cardioprotective properties[8]. However, it is unknown whether key characteristics of adipocytes remain the same or show tissue-specificity, depending on whether they reside in the adipose tissue or heart.

CVDs, such as coronary artery disease (CAD) and heart failure (HF), are the major causes of mortality and morbidity worldwide[9]. Epicardial fat has been suggested to be associated with CVDs[8]. Epicardial fat volume is associated with type 2 diabetes (T2D), HF, and atrial fibrillation[10]. It has also been reported that heart and coronary arteries are affected by epicardial adipose tissue through paracrine and vasocrine secretion of proinflammatory cytokines[11]. Epicardial adipose tissue obtained from patients with CAD shows increased expression of inflammatory cytokines[12]. In addition, this study also found inflammatory cells in the epicardial adipose tissue[12]. However, less is known about heart adipocytes, and in general, it is unknown how gene regulatory mechanisms and cell signaling pathways regulate adipocytes in the heart versus adipose tissue and whether they contribute to various CVDs.

Single nucleus RNA-seq (snRNA-seq) has emerged as a powerful and innovative method to study the gene expression profiles of various cell-types in solid tissues[13]. Several studies have focused on identifying cellular and transcriptional diversity in heterogeneous solid tissues, such as human heart[14,6] and adipose tissue[15,16]. However, genetic regulation and gene expression profiles of adipocytes across tissues and the relevance of their potential tissue-specificity to the development of CVDs have remained elusive. Thus, it is not well understood whether heart adipocytes directly relate to CVDs. To address these knowledge gaps, we aimed to uncover the distinct, tissue-specific expression profiles of heart and adipose tissue resident adipocytes, pathways involved in their tissue-specificity, and their genetic links to CVDs.

Materials and Methods

Data availability

Access to the Finnish Twin[17] and CRYO[18,19] adipose snRNA-seq data are described in the original publications for each cohort. Access to the human heart snRNA-seq data[6] is available from Broad Institute's Single Cell Portal (https://singlecell.broadinstitute.org/single_cell) under study ID SCP498. GTEx eGenes data, for adipose subcutaneous, heart atrial appendage, and heart LV, are available in GTEx portal v.8. All data supporting the

findings of this study are available within this article and its accompanying files. Please see the Major Resources Table in the Supplemental Materials.

snRNA-seq cohort of human subcutaneous adipose tissue

To investigate the tissue-specific expression profile of adipocytes, we used previously generated snRNA-seq data from a human subcutaneous adipose tissue study sample, as described in detail earlier[15]. Briefly, the 15 participants included in this snRNA-seq study sample were recruited at the University of Helsinki, Finland. The individuals (nine females and six males) underwent subcutaneous adipose biopsies as part of the Finnish Twin study[17] (7 individuals) and CRYO study[18,19] (8 individuals). The mean age and body mass index (BMI) of the participants are 32.70 ± 7.12 years and 31.45 ± 5.42 kg/m^2, respectively. Both studies were approved by the Ethics Committee of the Hospital District of Helsinki and Uusimaa. All participants provided written informed consent to participate in these studies. All research was performed in alignment with the principles of the Helsinki Declaration. Isolation and processing (library construction and sequencing) of nuclei were described in detail in Pan *et al*[15].

snRNA-seq cohort of adult human heart tissue

For cross-tissue comparisons of the gene expression profiles of adipocytes, we analyzed an adult human myocardial tissue cohort with snRNA-seq data[6]. In this previously published cohort, the myocardial tissue samples were collected from 7 deceased transplant donors (four females and three males) with a mean age of 51.71±7.2 years and BMI of 23.5±3.1 kg/m^2, respectively. None of the donors had any clinical evidence of cardiac dysfunction. Tissues were collected from the lateral aspect of the four heart chambers (RA, LA, RV, and LV). The human heart snRNA-seq study was approved by the institutional review boards at the Gift-of-Life Donor Program, the University of Pennsylvania, Massachusetts General Hospital, and the Broad Institute. Written informed consent for the heart snRNA-seq study was obtained from the next of kin of all donors. We downloaded the human heart snRNA-seq data[6] from Broad Institute Single Cell Portal. Of the two replicates, we used second replicate to reduce heterogeneity as the samples were processed differently in terms of the reverse transcription[6].

Processing and analyzing the subcutaneous adipose snRNA-seq data

Alignment and quality control—We used STARsolo[20] for read alignment and gene quantification of the subcutaneous adipose tissue snRNA-seq data. Data alignment was performed using the human reference genome GRCh38. For generating counts for both pre-mRNA and exonic RNA, “-soloFeatures GeneFull” command was employed. To remove empty and contaminated droplets, we applied the Debris Identification using Expectation Maximization (DIEM) approach[21]. To ensure that all barcodes correspond to true nuclei, we performed standard quality control (QC)[15], and filtered the droplets based on three QC metrics using the following exclusion criteria: (a) the number of Unique Molecular Identifiers (UMIs) (UMI<200 and UMI>20,000); (b) the number of genes (genes<200); and (c) the percentage of reads mapped to the mitochondrial genome (mitochondrial counts>10).

Normalization and integration—We normalized the data using the SCTransform function of the Seurat v4.0.3[22] and then applied the Seurat integration workflow for the normalized data. Briefly, we selected a set of 2,500 most variable features (genes) using SelectIntegrationFeature function and prepared the SCTransformed expression matrix for these selected genes using PrepSCTIntegration function. Finally, we performed integration using FindIntegrationAnchors and IntegrateData functions.

Dimensionality reduction and clustering—We performed principal component analysis (PCA) of the integrated data using the RunPCA function of the Seurat v4.0.3[22] and calculated the first 50 principal components. Clustering was performed using FindNeighbors function (based on k-nearest neighbor (KNN) graphs) and FindClusters function (Louvain algorithm) with dimensions 1–30. We applied a resolution of 0.7 to classify the nuclei into clusters. To represent the data in two-dimensional space, we performed nonlinear dimensional reduction using Uniform Manifold Approximation and Projection (UMAP)[23].

Cell-type annotation—For cell-type assignment, we used the cell-type annotation tool SingleR v1.4.1[24]. SingleR determines the cellular identity of each cluster based on the reference datasets of pure cell types sequenced by either RNA-seq or microarray technology. We used manually annotated human subcutaneous adipose snRNA-seq data[15] (n=15) and an immune cell-type specific RNA-seq dataset, 'Database for Immune Cell Expression' (n=1,561), available in the SingleR package[24] as reference data sets. Droplets with ambiguous assignments were removed separately.

Marker gene identification—We identified the marker genes for each cluster with FindAllMarkers function in Seurat v4.0.3[22]. This function uses the Wilcoxon rank sum test (by default) with a $\log_2$ fold change threshold of 0.25. Genes that are detected in a minimum fraction of 25% nuclei (min.pct=0.25) were tested for marker gene identification. Bonferroni corrected $p<0.05$ was considered statistically significant.

Processing and analyzing the heart snRNA-seq data

Normalization and integration—For the processing of heart snRNA-seq data, we performed a similar workflow as described above for the subcutaneous adipose snRNA-seq data. Briefly, count data of each heart chamber (RA, LA, RV, and LV) was normalized using the SCTransform function of Seurat v4.0.3[22]. Normalized dataset for each chamber was processed separately using Seurat[22] functions SelectIntegrationFeature, PrepSCTIntegration, FindIntegrationAnchors, and IntegrateData.

Dimensionality reduction and clustering—Dataset for each heart chamber was then subjected to dimensionality reduction using PCA. Clustering was performed using FindNeighbors function (top 15 PCA vectors) and FindClusters function (resolution 0.5). Finally, UMAPs for all the chambers were created using RunUMAP function.

Cell-type annotation and marker gene identification—To annotate cell types for each chamber of the heart, we used the automated cell-type cluster annotation tool SingleR v1.4.1[24] with an independent human heart dataset[25] as a reference while removing the

droplets with ambiguous assignments. After the cell type annotation, we identified the cell-type marker genes for each heart chamber using Seurat[22], as described above for the subcutaneous adipose snRNA-seq. Noteworthy, using the single nucleus RNA-seq data we cannot directly identify adipose tissue per se in the heart, rather we identify adipocytes that is a unique cell-type of the adipose tissue.

Pathway enrichment analysis for adipocyte marker genes

We used a web-based tool WebGestalt[26] to perform pathway enrichment analysis of the five sets of adipocyte marker genes (adipocyte marker genes for RA, LA, RV, LV, and subcutaneous adipose tissue). WebGestalt implements a hypergeometric test to identify an over-representation of a set of genes among all the genes in a specific KEGG pathway. Only the expressed genes were used as a reference gene set for each pathway enrichment analysis. KEGG pathway with adjusted $p<0.05$ was defined as statistically significant. We used the Seurat[22] function DotPlot to compare the average expression of pathway genes across the cell-types in LA and RA using all available atrium samples (n=6 for LA and n=5 for RA)[6]. Visualization of the pathway genes within the KEGG pathway was performed using the pathview[27] R package.

Module score analysis

To calculate the module scores for pathway-specific gene modules, we used AddModuleScore function in Seurat v4.0.3[28]. This function estimates the module scores by calculating the difference between the average expression level of genes within the module compared to aggregated expression of control gene sets. Pathway-specific adipocyte marker genes were used as input. Based on the mean expression, genes of interest were binned into 24 bins. Control gene sets were randomly selected from each bin. To further investigate the significance of the module score difference between adipocytes and non-adipocytes in both tissues, we first down-sampled the nuclei by a factor of 50 and then performed permutation tests one million times by preserving the proportion of adipocytes and non-adipocytes.

Transcription factor enrichment analysis

We performed transcription factor (TF) analysis using the Enrichr online tool[29]. Entrez gene symbols of five sets of genes (unique adipocyte marker genes for RA, LA, RV, LV, and subcutaneous adipose tissue) were used as input data to identify the TFs that regulate the expression of these genes. For enrichment analysis, we used Chip Enrichment Analysis (ChEA) database[30]. ChEA contains results of TF targets from published ChIP-seq studies. Enrichr computes p-values for each TF using the Fisher exact test. For correction of multiple testing, FDR<0.05 was applied.

Gene set enrichment analysis for diseases associations

Since the 7 heart snRNA-seq samples were taken from patients with no clinical evidence of cardiac dysfunction, we could not directly assess them for CAD or HF in our study. Therefore, we leveraged the identified heart adipocyte marker genes to determine the role of local variants of these marker genes for enriched associations with CAD and HF in the previous extensive CAD and HF genome-wide association studies (GWASs)[31,32].

Accordingly, we used MAGENTA[33] to identify whether local variants (see below) within each set of adipocyte marker genes are enriched for associations with CAD or HF. MAGENTA is a multivariate linear regression-based method that tests the enrichment of sets of functionally related genes with polygenic traits or diseases using summary statistics of GWAS. Briefly, MAGENTA (a) maps the chromosomal position and *p*-value of GWAS SNPs onto genes; (b) scores the genes based on local SNPs; (c) corrects gene scores for confounding factors such as SNP number, gene size, and linkage disequilibrium (LD); and (d) calculates enrichment *p*-value for each gene set of interest.

To test the association of chamber-specific adipocyte marker genes with CVDs, we used publicly available summary statistics of two GWAS studies. The first study is a CAD meta-analysis[31], which consisted of 42,335 CAD patients and 78,240 control individuals (a total of 120,575 individuals) from 20 individual studies. Summary statistics for the CAD meta-analysis study[31] was downloaded from the project website. The second study is the HF GWAS meta-analysis[32], which was performed across 26 individual studies from the HERMES Consortium. This meta-analysis comprises of a total of 977,323 European descent individuals, including 47,309 HF patients and 930,014 healthy controls. Summary statistics of the HF GWAS were downloaded from the HERMES project website.

For enrichment analysis, we used gene boundaries of 500 kb upstream and 500 kb downstream of the transcription start site and end of the gene, respectively. Due to the high gene density and tight linkage disequilibrium (LD) in the HLA region, we removed the genes that reside in the HLA region (default settings). Enrichment *p*-values were corrected for multiple testing using FDR<0.05.

Cis-expression quantitative trait locus (eQTL) analysis

To identify *cis*-eQTLs, defined here as DNA variants that regulate the expression of a near-by genes, for adipocyte marker genes across both tissues, we used three sets of data: (a) adipose subcutaneous eGenes, (b) heart atrial appendage eGenes, and (c) heart LV eGenes from Genotype-Tissue Expression (GTEx) portal v.8[34]. We first filtered each dataset to only include *cis*-eQTL SNPs with a minor allele frequency (MAF) of more than 5% in the GTEx data and permuted *p*-value<0.05. We selected the MAF more than 5% cut point to focus on commonly enough variants in the relatively small GTEx RNA-seq data sets. The permutation *p*-values were calculated using the FastQTL tool to test for the associations of the *cis*-eQTL variants with the expression of the corresponding genes, as described earlier[34] and reported in the publicly available GTEx *cis*-eQTL results at the GTEx portal. The GTEx participants are 85% White, which reflects relatively well our study participants who are White. We then identified *cis*-eQTL variants regulating tissue-specific and tissue-shared adipocyte marker genes between subcutaneous adipose tissue and each chamber of the heart (RA, LA, RV, and LV). To find the significant associations (*p*-value<5×10^{-8}) between eQTL variants and CVD traits, we used the cardiovascular disease knowledge portal (CVDKP) data (November 9, 2022, date last accessed).

Cell-cell communication analysis of subcutaneous adipose tissue and heart

To identify cell-cell communication in subcutaneous adipose tissue and each of the heart chambers (RA, LA, RV, and LV), we used the intercellular communication analysis tool, CellChat[35]. CellChat uses gene expression information from single-cell or snRNA-seq data and models the probability of intercellular communication by integrating gene expression information and prior knowledge of ligand-receptor (L-R) interactions. CellChat then predicts incoming and outgoing cell-cell communication using network analysis and pattern recognition approach. CellChat uses a one-sided permutation test to identify the significant interactions between two cell-types. Interactions with $p<0.05$ are considered as statistically significant. We applied CellChat to our subcutaneous adipose tissue and heart datasets, and performed L-R interaction analysis using the standard CellChat analysis workflow with default settings. Next, we compared significant L-R interactions between subcutaneous adipose tissue and each of the heart chambers to identify tissue-specific adipocyte-associated L-R interactions and their corresponding signaling pathways.

Results

Single nucleus RNA-seq analysis of subcutaneous adipose tissue and heart reveals tissue-resident and tissue-shared adipocyte marker genes

Our study design to identify subcutaneous adipose tissue and heart -specific adipocytes and their profiles is illustrated in Figure 1A,B. To investigate tissue-specific expression profiles of adipocytes, we used previously reported snRNA-seq datasets of human subcutaneous adipose[15] and heart[6]. For subcutaneous adipose tissue, snRNAseq data were first aligned to the human reference genome and filtered for standard QC (see Methods). Following QC, the total number of nuclei in the subcutaneous adipose tissue dataset was 37,865. We then performed clustering and cell-type assignment to identify cell-types in subcutaneous adipose tissue (Figure 1A). Assigned cell-types in subcutaneous adipose tissue dataset included adipocytes, preadipocytes, fibroblasts, myeloid, endothelial cells, perivascular, B cells, T cells, lymphatic endothelial cells, mast cells, and natural killer T cells (Figure 1C). For the heart snRNA-seq data, we performed clustering and cell-type annotation (Figure 1A) of each heart chamber (RA, LA, RV, and LV) separately (see Methods). The total number of nuclei in RA, LA, RV, and LV were 41,204, 42,867, 28,696, and 39,639, respectively. We observed ten heart cell-types, which included cardiomyocytes, fibroblasts, endothelial, mesothelial, myeloid, adipocytes, neuronal, pericytes, smooth muscle cells, and lymphoid cells (Figure 1D–G). We use the term heart or chamber-based adipocytes for the adipocytes observed in the heart. To exemplify the adipocyte cluster among all subcutaneous adipose and heart cell-type clusters, the expression of an adipocyte marker gene *GPAM* is shown in the UMAP visualization of subcutaneous adipose tissue and all heart chambers (Figure S1A–E).

As the snRNAseq data analysis of both tissues confirmed the presence of adipocyte clusters in subcutaneous adipose tissue and each of the heart chambers, we next investigated whether adipocytes in both tissues express the same sets of adipocyte marker genes, and thus comprise tissue-shared or tissue-resident expression profiles. To test this, we first identified adipocyte-specific marker genes in the subcutaneous adipose tissue and heart. These adipocyte marker genes are defined as genes that are expressed specifically in

adipocytes when compared to other cell-types (see Methods). We found 207 adipocyte marker genes in the subcutaneous adipose tissue, and 214, 240, 115, and 256 adipocyte marker genes in RA, LA, RV, and LV, respectively. The adipocyte marker genes of the subcutaneous adipose tissue and each heart chamber (RA, LA, RV, and LV) are listed in Table S1–S5.

We next investigated whether the adipocyte marker genes are shared between the subcutaneous adipose tissue and each heart chamber (RA, LA, RV, and LV). Adipocyte marker genes that were specifically present in one tissue but absent in the other were identified as tissue-resident adipocyte marker genes (Figure 2A). We found 75 adipocyte marker genes that were shared by both subcutaneous adipose tissue and RA, while 139 adipocyte marker genes were only present in the RA and 132 unique adipocyte marker genes in subcutaneous adipose tissue (Figure 2B). Similarly, we found 162, 63, and 170 unique adipocyte marker genes in LA, RV, and LV, respectively, when compared with adipocyte marker genes in subcutaneous adipose tissue (Figure 2C–E). Taken together, these comparisons of the adipocyte marker genes between tissues indicate that the majority (~60–70%) of the adipocyte marker genes are tissue-resident. Thus, these unique adipocyte marker genes in each tissue might be involved in distinct molecular mechanisms in adipocyte function of the particular tissue.

Comparisons of the adipocyte marker genes between the subcutaneous tissue and heart chambers identify distinct functional pathways in the human heart

To underpin the functional pathways regulated by the tissue-resident adipocyte marker genes, we conducted the KEGG pathway enrichment analysis using WebGestalt[26]. We observed significant differences between pathways identified in the subcutaneous adipose tissue and each of the heart chambers (RA, LA, RV, and LV). Pathway enrichment analysis using heart-specific adipocyte marker genes identified a significant enrichment of the propanoate metabolism pathway (FDR<0.05), consistently in all four chambers separately (Figure 2B–E). Noteworthy, the propanoate metabolism pathway shows the highest enrichment ratio in all four heart chambers (Table S6–S9); however, this pathway is not enriched among the subcutaneous adipose tissue-resident adipocyte marker genes. We did not observe any significant functional pathways using unique adipocyte marker genes in the subcutaneous adipose tissue (Figure 2B–E); however, KEGG pathways analysis using all adipocyte marker genes (both shared and non-shared) resulted in the well-known adipose tissue pathways, including the insulin signaling pathway (Table S10). Insulin signaling pathway is also significantly enriched among all heart adipocyte marker genes (Figure 3), with some shared pathway genes observed across the two tissues, including *FASN* and *LIPE*. We also observed that *IRS2*, the loss of which has previously been linked to heart failure[36], is an adipocyte marker gene in all four chambers but not in the subcutaneous adipose tissue. Taken together, our pathway enrichment analyses indicate that the propanoate metabolism pathway is heart-specific and might be a key distinct functional pathway in heart resident adipocytes.

Comparisons of the adipocyte marker genes between the heart chambers show well-coordinated functional pathways at the chamber level

We also searched for differences in adipocyte marker genes between the heart chambers (RA, LA, RV, and LV) and found chamber-specific and chamber-shared adipocyte marker genes (Figure 3A). For example, 137 adipocyte marker genes were shared between RA and LA, while 77 adipocyte marker genes were only present in RA and 103 in LA. Thus, the adipocyte marker genes also demonstrate some chamber-specificity.

To further investigate the possible chamber-specific role of adipocytes, we performed the KEGG pathway enrichment analysis using all adipocyte marker genes in RA (n=214), LA (n=240), RV (n=115), and LV (n=256). We found that the adipocyte marker genes in both atriums are enriched for multiple shared functional pathways, which were not observed in the ventricles (Figure 3B), including the glyoxylate and dicarboxylate metabolism, glycerolipid metabolism, citrate cycle, carbon metabolism, biosynthesis of unsaturated fatty acids, and metabolic pathways. We also observed that the adipocyte marker genes in both ventricles are enriched for less functional pathways when compared to the atriums, majority of which overlap with the atrium pathways. To further evaluate whether the differences observed are due to intrinsic characteristics from adipocytes in different heart chambers or due to differences in other cell-types, we also compared myeloid marker genes and their functional pathways between the heart chambers. We did not observe similar functional coordination across atriums and ventricles as with the adipocyte marker genes when using the myeloid marker genes (Figure S2A–B), suggesting that the observed differences may be due to intrinsic characteristics of adipocytes in atriums and ventricles.

Module score analysis identifies tissue-specific drivers of the propanoate metabolism pathway

We next used the module score analysis to evaluate the tissue-specific profiles of propanoate metabolism pathway genes (Figure 4A–B). We performed these analyses on the UMAP representation of both subcutaneous adipose tissue and heart chambers. Module score analysis of propanoate metabolism pathway genes (Figure 4B) comparing the average expression of the propanoate metabolism pathway genes in the LA adipocytes versus other heart cell-types and subcutaneous adipose tissue adipocytes versus other adipose cell-types (see Methods) revealed a strong expression enrichment of these pathway genes in the LA adipocytes (Figure 4C–F). Next, similar module score analyses were performed for the adipocyte cluster in subcutaneous adipose tissue and the other three heart chambers. These module score analyses also suggest that the genes of the propanoate metabolism pathway are more strongly enriched for adipocytes in the other three chambers (RV, LV, and RA) (Figure S3A–C), than for the adipocytes in the subcutaneous adipose tissue. In summary, in line with the pathway analyses, the module score results indicate that the expression profiles of the genes in the propanoate metabolism pathway are tissue-enriched in the adipocytes of the heart chambers.

Adipocytes in the heart and subcutaneous adipose tissue are enriched for binding of distinct transcription factors (TFs)

We next searched for transcription factors (TFs) that regulate tissue-resident adipocyte marker genes. We first performed TF enrichment analysis using the Enrichr tool[29] on the unique adipocyte marker genes in each heart chamber as well as the unique adipocyte marker genes in the subcutaneous adipose tissue. We identified significant TFs (FDR<0.05) that target adipocyte marker genes in each heart chamber and subcutaneous adipose tissue (Figure 4G). Among these TFs, SOX2 and CBP are identified as heart adipocyte-specific and enriched for all heart chambers. In addition to heart adipocyte-specific TFs, we observed three subcutaneous adipose tissue adipocyte-specific TFs, RUNX2, TRIM28, and HIF1A, which were enriched in at least three comparisons between subcutaneous adipose tissue and various heart chambers. Together, our finding suggests that these TFs might be essential to regulate the tissue-specific profiles of adipocytes.

CVD GWAS variants are enriched in the RA marker gene regions

We tested whether unique heart-specific adipocyte marker genes in each chamber are enriched for coronary heart disease (CAD) or heart failure (HF) genome-wide association study (GWAS) variants residing in their *cis*-regulatory regions (Table 1). We used MAGENTA[33] (see Methods) to test for the enrichment of CAD and HF GWAS associations in the following four gene sets: (a) 139 unique adipocyte marker genes in RA; (b) 63 unique adipocyte marker genes in RV; (c) 162 unique adipocyte marker genes in LA and (d) 170 unique adipocyte marker genes in LV.

We first tested for the enrichment of CAD GWAS variants in the *cis*-regions of the unique adipocyte markers genes of the four heart chambers using the summary level results of the CAD GWAS meta-analysis[31], comprising 42,335 CAD cases and 78,240 controls. We observed significant enrichment of CAD associations with the RA adipocyte marker gene regions (Table 1; $P_{RA}^{GSEA} = 0.0005$), passing the correction for multiple testing (adj $p<0.0062$; four gene sets and two disorders tested) (Table 1). We did not observe significant enrichment of CAD associations for adipocyte marker gene regions in RV ($P_{RV}^{GSEA} = 0.9130$), LA ($P_{LA}^{GSEA} = 0.359$), and LV ($P_{LV}^{GSEA} = 0.5470$) (Table 1).

We next tested for the enrichment of heart failure GWAS variants in the *cis*-regions of the unique adipocyte markers genes of the four heart chambers using the summary level results of the HERMES GWAS meta-analysis[32], comprising 47,309 heart failure cases and 930,014 healthy controls. RA- and LA-specific adipocyte marker genes were nominally enriched for heart failure associations with a *p*-value of 0.0312 and 0.0325 (Table 1). No enrichment of heart failure associations was observed with the LV and RV adipocyte marker genes.

Taken together, our GWAS enrichment analyses of the unique heart chamber marker gene regions provided significant support for the enrichment of CAD GWAS variants in the RA-specific adipocyte marker gene regions and suggestive support for the enrichment of heart failure GWAS variants in the RA- and LA-specific adipocyte marker gene regions.

LA and RA show adipocyte-specific expression of seven propanoate metabolism pathway genes

As the unique adipocyte marker genes in LA and RA are enriched for CAD and HF GWAS risk variants, we next investigated whether the expression of the propanoate metabolism pathway genes is specific to adipocytes in both atriums using all available atrium samples (n=6 for LA and n=5 for RA)[6]. We used Seurat[22] function DotPlot to compare the average expression of the propanoate metabolism genes across the samples at the cell-type level. The results demonstrate that the key genes of the propanoate metabolism pathway, *ACACA, BCKDHB, ECHDC1, EHHADH, HIBCH, LDHA,* and *PCCA*, are predominantly only expressed in the human LA and RA adipocytes, with minimal expression in the other heart cell-types (Figure 5A–B). The central role of these seven propanoate metabolism genes in the KEGG pathway of propanoate metabolism is depicted in Figure S4. Together, our findings suggest that the expression of the seven propanoate metabolism pathway genes is specific to the adipocytes in the human LA and RA, indicating their important role in the propanoate metabolism of the human heart.

Cis-eQTL variants regulate tissue-resident adipocyte markers and propanoate metabolism pathway genes

To elucidate genetic regulation of the tissue-resident adipocytes, we searched for *cis*-eQTL variants that regulate unique adipocyte marker genes in the heart and subcutaneous adipose tissue using three sets of Genotype-Tissue Expression (GTEx) expression data (see Methods). Interestingly, we observed *cis*-eQTL variants that are associated with unique adipocyte marker genes of both subcutaneous adipose tissue and each of the heart chambers (Figure S5). Among the heart adipocyte marker gene the *cis*-eQTL variants, rs2744937 and rs3800461 regulate *C6orf106* that is a unique adipocyte marker gene in RA, LA, and LV. According to the Cardiovascular Disease Knowledge Portal (CVDKP) data, these *cis*-eQTL variants rs2744937 and rs3800461 are also significantly associated with CAD, resulting in *p*-values of 2.34×10^{-11} and 5.87×10^{-12}, respectively. In addition, we observed that the *cis*-eQTL variants rs291466 and rs16859711 regulate propanoate metabolism pathway genes *HIBCH* and *EHHADH*. Among these variants, rs291466 is also significantly associated with diastolic blood pressure (*p*-value=8.00×10^{-12}). Unique adipocyte marker gene *cis*-eQTL variants and their CVD GWAS associations are shown in Figure S5A–D.

Cell-cell communication analysis identifies specific heart adipocyte-associated ligand-receptor interactions and signaling pathways

To search for significant ligand-receptor (L-R) interactions and signaling differences among adipocytes and other cell-types in the subcutaneous adipose tissue and heart, we performed cellular communication analysis using CellChat[35]. We first compared the significant aggregated cell-cell communication networks we identified between each of the heart chambers (RA, LA, RV, and LV) and subcutaneous adipose tissue (Figure 6A). We observed a tissue-specific distinct communication structure in the subcutaneous adipose tissue when compared to the communication structures in the four heart chambers (Figure 6A). Moreover, we observed that the overall cell-cell communication structures are highly similar between RA and LA, and between RV and LV (Figure 6A), respectively. In total,

there are 59 adipocyte-associated ligand-receptors interactions in RA, 81 in LA, 18 in RV and 31 in LV, respectively. These overall cell-cell communication structures on one hand between the subcutaneous adipose tissue and heart, and on the other hand within the heart atriums versus ventricles are likely driven by distinct tissue-specific cell-type compositions.

We next searched for L-R interactions involving adipocytes in subcutaneous adipose tissue and each of the heart chambers. The L-R interactions where adipocytes are either sender and/or receiver cell-type were considered as adipocyte-associated L-R interactions. We first identified adipocyte-associated L-R interactions in subcutaneous adipose tissue and heart and then investigated whether any of these L-R interactions are shared between both tissues. We found 27, 17, 12, and 18 non-shared adipocyte-associated L-R interactions in RA, LA, RV, and LV, respectively, when compared with adipocyte-associated L-R interactions in subcutaneous adipose tissue (Table S11–S14). Among the adipocyte-associated L-R interactions in the heart chambers, four L-R interactions (EFNA5-EPHA4, EFNA5-EPHA3, THBS1-CD36, and IGF1-IGF1R) are shared across all four heart chambers; however, none of these interactions were observed among the adipocyte-associated L-R interactions in the subcutaneous adipose tissue (Figure 6B). The signaling pathways associated with these L-R interactions are EPHA, THBS, and IGF. In addition, we observed three adipocyte-associated L-R interactions (SEMA3C-NRP2-PLXNA2, LAMA4-ITGA6-ITGB1, LAMC1-ITGA6-ITGB1) only present in the subcutaneous adipose tissue (Figure S6H–J) but not in the heart. Taken together these cellular communication results between the subcutaneous adipose tissue and heart revealed 22 distinct heart adipocyte-associated L-R pairs and signaling pathways, which likely contribute to the regulation of the observed heart-specific profiles of adipocytes.

Taken together our results identify the propanoate metabolism pathway as a novel distinct characteristic of the heart-resident adipocytes, and discover a significant enrichment of CAD GWAS risk variants among the unique RA adipocyte marker genes. Thus, we introduce a new function and genetic link to CAD for the previously unexplored heart-resident adipocytes.

Discussion

We present a cross-tissue analysis of adipocyte cell populations, comparing their subcutaneous adipose and heart single-nucleus transcriptomes to identify distinct tissue-specific expression profiles of adipocytes, their functional pathways and gene regulatory mechanisms with potential therapeutic application for CVDs. By analyzing the subcutaneous adipose tissue and heart snRNA-seq data, we identify novel tissue-resident adipocyte marker genes. Using these unique adipocyte marker genes, we discover distinct functional pathways, transcription factors, and *cis*-eQTL variants that characterize tissue-specific profiles of adipocytes. Furthermore, our genetic results reveal enrichments of heart-resident adipocyte marker genes for CAD and HF GWAS risk variants, suggesting potential therapeutic target genes for CVDs.

Our pathway enrichment analyses reveal a significant enrichment of the propanoate metabolism pathway among the tissue-resident adipocyte marker genes in all heart

chambers. This pathway involves propionate, a short chain fatty acid, which is derived from several sources including the metabolism of intestinal bacteria and diet[37]. A previous study has shown that gut microbiota-derived propionate has cholesterol-lowering and atheroprotective properties[38]. The concentration of propionate is also significantly altered in obesity[37,39,40], which is known to associate with CVDs, suggesting that propionate could have a critical effect on cardiac metabolism and function. Furthermore, a rat study by Wang et al. reported that propionate switches the fuel preference of heart from fatty acids to glucose[37], and thus the propionate metabolism may act as a linking pathway in cardiac energetics between the two fuel sources. A recent study also demonstrated that propionate protects the heart from damage, such as cardiac fibrosis, hypertrophy, and vascular dysfunction[41], and that propionate treatment significantly reduces atherosclerosis[41]. Our new findings as well as previous reports endorse the possibility that the propanoate metabolism pathway is heart adipocyte-specific and plays an important role in heart-resident adipocytes.

Our comparisons of pathway enrichment results between the heart chambers further demonstrate that the adipocyte-specific expression profiles of both atriums are enriched for multiple shared functional pathways (Figure 3B), which are not observed in the ventricles. Interestingly, the glycerolipid pathway gene, *DGAT2*, plays a key role in cardiac triglyceride synthesis[42]. A mice study also found that the expression of *LPIN1*, another gene of glycerolipid metabolism, is significantly decreased in individuals with heart failure[43]. Intermediates of citrate cycle, which is only shared by atriums (Figure 3B), are involved in cardioprotection[44]. As the previous studies indicate the involvement of these pathways and their genes in heart-specific molecular mechanism, the pathways we identified in the adipocytes of heart atriums might be important in the regulation of atrium adipocytes.

We also found that average expression of genes (*ECHDC1*, *ACACA*, *PCCA*, *BCKDHB*, *EHHADH*, *HIBCH*, and *LDHA*) of the propanoate metabolism pathway are enriched in the adipocyte clusters among all cell-types in the four heart chambers using a module score analysis. Previous work has reported the involvement of these genes in various cardiovascular events. The expression of *ECHDC1* is known to be elevated in myocardial tissue in patients with hypertrophic cardiomyopathy[45]. Upregulation of *ACACA* has been shown in the atrial myocardium of high-fat diet mice[46]. Another study on adult-onset dilated cardiomyopathy found compound heterozygous variants in the *PCCA* gene[47]. A mouse study by Dai *et al.* reported that the expression of *LDHA* is increased in the heart in response to hemodynamic stress[48]. Taken together, we show that these propanoate metabolism pathway genes that have been implicated in prior studies for their critical role in myocardial tissue are highly expressed only in heart adipocytes among all heart cell-types, although we recognize that further studies are warranted to determine the exact function of these genes in heart-resident adipocytes.

We observed notable differences in transcription factor bindings between subcutaneous adipose tissue and all four heart chambers. Among the heart adipocyte marker gene-specific TFs, SOX2 is a well-studied TF that is crucial for lineage determination in human mesenchymal stem cells[49]. Previous studies showed that SOX2 improves the cardiovascular repair capacity of mesoangioblasts in the acute myocardial infarction model[50]. We also

found another heart adipocyte-aware TF, CREB binding protein (CBP) that is known to interact with other TFs and is involved in cardiac hyperthrophy[51]. In addition, we identified multiple adipose tissue adipocyte-specific TFs that included RUNX2, TRIM28, and HIF1A. Previous works reported that RUNX2 is highly expressed in growth-arrested preadipocytes[52] and it is known to have an inhibitory role in adipocyte differentiation. TRIM28 is a crucial regulator of adipose tissue function, loss of which promotes obesity in mice[53]. HIF1A, the master regulator of cellular oxygen homeostasis, promotes obesity-induced inflammation in adipose tissue hypoxia[54]. Therefore, as these previous findings indicate that TFs can have significant involvement in various tissue-specific molecular mechanisms, the TFs we identified in heart-resident adipocytes, SOX2 and CBP, can similarly also have important roles in heart-specific functions.

Adipose tissue-resident adipocytes play an important role in metabolic regulation, and dysfunctional adipocytes are known to be associated with several CVDs[55,56]. However, it is unknown how heart-resident adipocytes contribute to CVDs including CAD and HF. Using the MAGENTA GSEA approach, we discovered that RA-specific adipocyte marker genes are significantly enriched for CAD GWAS variants (adjusted $p<0.05$). Previous studies have demonstrated that RA impairment is an independent risk factor for acute myocardial infarction[57]. In addition, we identified an enrichment of RA- and LA-specific adipocyte marker genes for HF GWAS variants (unadjusted $p<0.05$). Based on these CAD and HF GWAS variant enrichments, we further demonstrate that the key propanoate metabolism pathway genes show adipocyte-specific expression in LA and RA. Our pathway enrichment analysis further showed that the LA-resident adipocyte marker genes are enriched for a valine, leucine, and isoleucine degradation pathway. Previous studies have reported that catabolic defects in these branched-chain amino acids (valine, leucine, and isoleucine) significantly contribute to the pathogenesis of HF[58]. The LA is often considered as a biomarker for risk prediction in various CVDs[59]. Taken together, our results provide new genetic evidence for the involvement of the identified RA-specific and LA-specific adipocyte marker genes in CAD and HF, and future in-depth investigations of these genes may yield novel therapeutic targets.

In our cellular communication analysis, we observed heart-specific adipocyte-associated L-R interactions and their signaling pathways. We found that adipocytes act as senders in the EPHA signaling in all heart chambers (Figure 6C,D and Figure S6A,B). We also found that adipocytes express the IGF1 ligand and communicate with cardiomyocytes in all heart chambers via the IGF1R receptor (Figure 6F and Figure S6D). IGF1 is known to play multiple key functional roles in the heart, including metabolism, autophagy, hypertrophy, contractility, and senescence[60]. In the THBS1-CD36 interaction, adipocytes act as receivers from myeloid cell-types in all heart chambers (Figure 6E and Figure S6C). CD36 is a multifunctional receptor, which is involved in the fatty acid uptake in myocardial tissue[61]. Interestingly, a previous study also reported that CD36 is associated with cardiovascular disease progression[62]. Among the identified L-R interactions in the heart chambers, NAMPT-INSR is the only L-R pair where the heart adipocytes act both as senders and receivers. NAMPT or VISFATIN is an adipokine that is previously known to be preferentially produced by the visceral adipose tissue[63]; yet we identify it to be expressed in the heart adipocytes and function in this L-R here. A prior study also found

that the level of epicardial NAMPT is increased in patients with CAD, when compared with control individuals' levels[64]. Therefore, based on the key L-R findings reported here and published earlier, it seems that the discovered heart adipocyte-associated ligands and receptors may contribute to the regulation of the heart-specific function of adipocytes and possibly link them to CAD. Our comparisons between the chambers also suggest chamber level coordination of heart adipocyte expression profiles as we observed a larger number of significant adipocyte-associated ligand-receptor interactions and functional pathways in the atriums than ventricles.

In addition to these new heart adipocyte findings, our study also has some limitations. First, all participants of this study were of European descent, preventing direct generalizations to other populations and warranting cross-tissue comparisons of adipocytes using samples from other, more diverse ancestries in the future. Second, the cohort sizes of subcutaneous adipose tissue (n=15) and heart (n=7) are relatively small. Larger snRNA-seq sample sizes may provide additional information about the expression of marker genes in adipocyte subtypes. Third, we used snRNA-seq datasets of heart and subcutaneous adipose tissue for our analysis. Inclusion of snRNA-seq data from visceral adipose tissue, would provide gene expression profiles of adipocytes in this other metabolically important fat depot, and thus investigations of adipocytes in other tissues warrant future studies. Fourth, in the GTEx portal there are bulk expression data available only in the LV out of the two ventricles. Therefore, we used the LV bulk expression data for the *cis*-eQTL analysis of the left and right ventricles while recognizing that the *cis*-eQTL analysis of the other chambers requires generation of new heart bulk RNA-seq data. Fifth, we recognize that it is possible that differences in participants' age and BMI between the subcutaneous adipose tissue and heart snRNAseq cohorts may also affect the results.

Taken together, our results contribute to the growing field of cardiac adiposity by identifying heart-resident adipocyte marker genes, and elucidating their functional pathways, and genetic links to CVDs. We identify the propanoate metabolism pathway to be enriched among the marker genes of the heart-resident adipocytes, consistently in all four chambers. We also discover a larger number of adipocyte-associated ligand-receptor interactions and functional pathways in the atriums than ventricles, suggesting chamber level coordination of adipocyte expression profiles. We further show that variants in the heart-resident adipocyte marker genes and their *cis* regulatory regions are enriched for associations with CAD and HF in previous extensive GWAS studies[31,32]. Thus, our results link variants in the identified novel heart-resident adipocyte marker genes to the increased genetic risk of CAD and HF.

Supplementary Material

Refer to Web version on PubMed Central for supplementary material.

Acknowledgments

We thank the individuals who participated in the Finnish Twin[17] and CRYO[18,19] adipose snRNA-seq study. The GTEx data used for the analyses described in this manuscript were obtained from the GTEx Portal on June 6, 2021.

Sources of funding

The work was supported by NIH grants R01HG010505 and R01DK132775. K.H.P. was funded by the Academy of Finland, grant numbers 335443, 314383, 272376, 266286; Finnish Medical Foundation; Gyllenberg Foundation; Novo Nordisk Foundation, grant numbers NNF20OC0060547, NNF17OC0027232, NNF10OC1013354; Finnish Diabetes Research Foundation; Sigrid Juselius Foundation, University of Helsinki and Helsinki University Hospital Government Research Funds. GTEx project was supported by the Common Fund of the Office of the Director of the National Institutes of Health, and by NCI, NHGRI, NHLBI, NIDA, NIMH, and NINDS.

Nonstandard Abbreviations and Acronyms

BMI	body mass index
CAD	coronary artery disease
CBP	CREB binding protein
ChEA	Chip Enrichment Analysis
CVD	cardiovascular disease
CVDKP	Cardiovascular Disease Knowledge Portal
DIEM	Debris Identification using Expectation Maximization
eQTL	expression quantitative trait locus
GTEx	Genotype-Tissue Expression
GWAS	genome-wide association study
HF	heart failure
KNN	k-nearest neighbor
LA	left atrium
LD	linkage disequilibrium
L-R	ligand-receptor
LV	left ventricle
MAF	minor allele frequency
MSC	mesenchymal stem cells
PCA	principal component analysis
QC	quality control
RA	right atrium
RV	right ventricle
snRNA-seq	single nucleus RNA-sequencing
T2D	type 2 diabetes

TF	transcription factor
UMAP	Uniform Manifold Approximation and Projection
UMI	Unique Molecular Identifier

References

1. Sonawane AR, Platig J, Fagny M, Chen CY, Paulson JN, Lopes-Ramos CM, DeMeo DL, Quackenbush J, Glass K, Kuijjer ML. Understanding Tissue-Specific Gene Regulation. Cell Rep. 2017;21:1077–1088. doi:10.1016/j.celrep.2017.10.001 [PubMed: 29069589]
2. Eraslan G, Drokhlyansky E, Anand S, Fiskin E, Subramanian A, Slyper M, Wang J, van Wittenberghe N, Rouhana JM, Waldman J, et al. Single-nucleus cross-tissue molecular reference maps toward understanding disease gene function. Science (1979). 2022;376:eabl4290. doi:10.1126/science.abl4290
3. Li SN, Wu JF. TGF-β/SMAD signaling regulation of mesenchymal stem cells in adipocyte commitment. Stem Cell Res Ther. 2020;11:41. doi:10.1186/s13287-020-1552-y [PubMed: 31996252]
4. Choe SS, Huh JY, Hwang IJ, Kim JI, Kim JB. Adipose Tissue Remodeling: Its Role in Energy Metabolism and Metabolic Disorders. Front Endocrinol (Lausanne). 2016;7:30. doi:10.3389/fendo.2016.00030 [PubMed: 27148161]
5. Longo M, Zatterale F, Naderi J, Parrillo L, Formisano P, Raciti GA, Beguinot F, Miele C. Adipose Tissue Dysfunction as Determinant of Obesity-Associated Metabolic Complications. Int J Mol Sci. 2019;20:2358. doi:10.3390/ijms20092358 [PubMed: 31085992]
6. Tucker NR, Chaffin M, Fleming SJ, Hall AW, Parsons VA, Bedi KC, Akkad AD, Herndon CN, Arduini A, Papangeli I, et al. Transcriptional and Cellular Diversity of the Human Heart. Circulation. 2020;142:466–482. doi:10.1161/CIRCULATIONAHA.119.045401 [PubMed: 32403949]
7. Corradi D, Maestri R, Callegari S, Pastori P, Goldoni M, Luong TV, Bordi C. The ventricular epicardial fat is related to the myocardial mass in normal, ischemic and hypertrophic hearts. Cardiovasc Pathol. 2004;13:313–316. doi:10.1016/j.carpath.2004.08.005 [PubMed: 15556777]
8. Iacobellis G, Bianco AC. Epicardial adipose tissue: emerging physiological, pathophysiological and clinical features. Trends Endocrinol. Metab. 2011;22:450–457. doi:10.1016/j.tem.2011.07.003 [PubMed: 21852149]
9. Bugiardini R, Cenko E. Sex differences in myocardial infarction deaths. The Lancet. 2020;396:72–73. doi:10.1016/S0140-6736(20)31049-7
10. van Woerden G, Gorter TM, Westenbrink BD, Willems TP, van Veldhuisen DJ, Rienstra M. Epicardial fat in heart failure patients with mid-range and preserved ejection fraction. Eur J Heart Fail. 2018;20:1559–1566. doi:10.1002/ejhf.1283 [PubMed: 30070041]
11. Iacobellis G Epicardial adipose tissue in contemporary cardiology. Nat Rev Cardiol. 2022;19:593–606. doi:10.1038/s41569-022-00679-9 [PubMed: 35296869]
12. Mazurek T, Zhang L, Zalewski A, Mannion JD, Diehl JT, Arafat H, Sarov-Blat L, O'Brien S, Keiper EA, Johnson AG, et al. Human Epicardial Adipose Tissue Is a Source of Inflammatory Mediators. Circulation. 2003;108:2460–2466. doi:10.1161/01.CIR.0000099542.57313.C5 [PubMed: 14581396]
13. Grindberg R v., Yee-Greenbaum JL, McConnell MJ, Novotny M, O'Shaughnessy AL, Lambert GM, Araúzo-Bravo MJ, Lee J, Fishman M, Robbins GE, et al. RNA-sequencing from single nuclei. Proc Natl Acad Sci USA. 2013;110:19802–19807. doi:10.1073/pnas.1319700110 [PubMed: 24248345]
14. Koenig AL, Shchukina I, Amrute J, Andhey PS, Zaitsev K, Lai L, Bajpai G, Bredemeyer A, Smith G, Jones C, et al. Single-cell transcriptomics reveals cell-type-specific diversification in human heart failure. Nat Cardiovasc Res. 2022;1:263–280. doi:10.1038/s44161-022-00028-6 [PubMed: 35959412]

15. Pan DZ, Miao Z, Comenho C, Rajkumar S, Koka A, Lee SHT, Alvarez M, Kaminska D, Ko A, Sinsheimer JS, et al. Identification of TBX15 as an adipose master trans regulator of abdominal obesity genes. Genome Med. 2021;13:123. doi:10.1186/s13073-021-00939-2 [PubMed: 34340684]
16. Miao Z, Alvarez M, Ko A, Bhagat Y, Rahmani E, Jew B, Heinonen S, Muñoz-Hernandez LL, Herrera-Hernandez M, Aguilar-Salinas C, et al. The causal effect of obesity on prediabetes and insulin resistance reveals the important role of adipose tissue in insulin resistance. PLoS Genet. 2020;16:e1009018. doi:10.1371/journal.pgen.1009018 [PubMed: 32925908]
17. van der Kolk BW, Saari S, Lovric A, Arif M, Alvarez M, Ko A, Miao Z, Sahebekhtiari N, Muniandy M, Heinonen S, et al. Molecular pathways behind acquired obesity: Adipose tissue and skeletal muscle multiomics in monozygotic twin pairs discordant for BMI. Cell Rep Med. 2021;2:100226. doi:10.1016/j.xcrm.2021.100226 [PubMed: 33948567]
18. van der Kolk BW, Muniandy M, Kaminska D, Alvarez M, Ko A, Miao Z, Valsesia A, Langin D, Vaittinen M, Pääkkönen M, et al. Differential Mitochondrial Gene Expression in Adipose Tissue Following Weight Loss Induced by Diet or Bariatric Surgery. J Clin Endocrinol Metab. 2021;106:1312–1324. doi:10.1210/clinem/dgab072 [PubMed: 33560372]
19. Jokinen R, Rinnankoski-Tuikka R, Kaye S, Saarinen L, Heinonen S, Myöhänen M, Rappou E, Jukarainen S, Rissanen A, Pessia A, et al. Adipose tissue mitochondrial capacity associates with long-term weight loss success. Int J Obes. 2018;42:817–825. doi:10.1038/ijo.2017.299
20. Dobin A, Davis CA, Schlesinger F, Drenkow J, Zaleski C, Jha S, Batut P, Chaisson M, Gingeras TR. STAR: ultrafast universal RNA-seq aligner. Bioinformatics. 2013;29:15–21. doi:10.1093/bioinformatics/bts635 [PubMed: 23104886]
21. Alvarez M, Rahmani E, Jew B, Garske KM, Miao Z, Benhammou JN, Ye CJ, Pisegna JR, Pietiläinen KH, Halperin E, et al. Enhancing droplet-based single-nucleus RNA-seq resolution using the semi-supervised machine learning classifier DIEM. Sci Rep. 2020;10:11019. doi:10.1038/s41598-020-67513-5 [PubMed: 32620816]
22. Butler A, Hoffman P, Smibert P, Papalexi E, Satija R. Integrating single-cell transcriptomic data across different conditions, technologies, and species. Nat Biotechnol. 2018;36:411–420. doi:10.1038/nbt.4096 [PubMed: 29608179]
23. McInnes L, Healy J, Saul N, Großberger L. UMAP: Uniform Manifold Approximation and Projection. J Open Source Softw. 2018;3:861. doi:10.21105/joss.00861
24. Aran D, Looney AP, Liu L, Wu E, Fong V, Hsu A, Chak S, Naikawadi RP, Wolters PJ, Abate AR, et al. Reference-based analysis of lung single-cell sequencing reveals a transitional profibrotic macrophage. Nat Immunol. 2019;20:163–172. doi:10.1038/s41590-018-0276-y [PubMed: 30643263]
25. Litviňuková M, Talavera-López C, Maatz H, Reichart D, Worth CL, Lindberg EL, Kanda M, Polanski K, Heinig M, Lee M, et al. Cells of the adult human heart. Nature. 2020;588:466–472. doi:10.1038/s41586-020-2797-4 [PubMed: 32971526]
26. Wang J, Vasaikar S, Shi Z, Greer M, Zhang B. WebGestalt 2017: a more comprehensive, powerful, flexible and interactive gene set enrichment analysis toolkit. Nucleic Acids Res. 2017;45:W130–W137. doi:10.1093/nar/gkx356 [PubMed: 28472511]
27. Luo W, Brouwer C. Pathview: an R/Bioconductor package for pathway-based data integration and visualization. Bioinformatics. 2013;29:1830–1831. doi:10.1093/bioinformatics/btt285 [PubMed: 23740750]
28. Tirosh I, Izar B, Prakadan SM, Wadsworth MH, Treacy D, Trombetta JJ, Rotem A, Rodman C, Lian C, Murphy G, et al. Dissecting the multicellular ecosystem of metastatic melanoma by single-cell RNA-seq. Science (1979). 2016;352:189–196. doi:10.1126/science.aad0501
29. Kuleshov MV, Jones MR, Rouillard AD, Fernandez NF, Duan Q, Wang Z, Koplev S, Jenkins SL, Jagodnik KM, Lachmann A, et al. Enrichr: a comprehensive gene set enrichment analysis web server 2016 update. Nucleic Acids Res. 2016;44:W90–W97. doi:10.1093/nar/gkw377 [PubMed: 27141961]
30. Lachmann A, Xu H, Krishnan J, Berger SI, Mazloom AR, Ma'ayan A. ChEA: transcription factor regulation inferred from integrating genome-wide ChIP-X experiments. Bioinformatics. 2010;26:2438–2444. doi:10.1093/bioinformatics/btq466 [PubMed: 20709693]

31. Stitziel NO, Stirrups KE, Masca NGD, Erdmann J, Ferrario PG, König IR, Weeke PE, Webb TR, Auer PL, Schick UM, et al. Coding Variation in ANGPTL4, LPL, and SVEP1 and the Risk of Coronary Disease. N Engl J Med. 2016;374:1134–1144. doi:10.1056/NEJMoa1507652 [PubMed: 26934567]
32. Shah S, Henry A, Roselli C, Lin H, Sveinbjörnsson G, Fatemifar G, Hedman ÅK, Wilk JB, Morley MP, Chaffin MD, et al. Genome-wide association and Mendelian randomisation analysis provide insights into the pathogenesis of heart failure. Nat Commun. 2020;11:163. doi:10.1038/s41467-019-13690-5 [PubMed: 31919418]
33. Segrè AV, Groop L, Mootha VK, Daly MJ, Altshuler D. Common Inherited Variation in Mitochondrial Genes Is Not Enriched for Associations with Type 2 Diabetes or Related Glycemic Traits. PLoS Genet. 2010;6:e1001058. doi:10.1371/journal.pgen.1001058 [PubMed: 20714348]
34. The GTEx Consortium, The GTEx Consortium atlas of genetic regulatory effects across human tissues. Science. 2020;369:1318–1330. doi: 10.1126/science.aaz1776. [PubMed: 32913098]
35. Jin S, Guerrero-Juarez CF, Zhang L, Chang I, Ramos R, Kuan CH, Myung P, Plikus MV., Nie Q. Inference and analysis of cell-cell communication using CellChat. Nat Commun. 2021;12:1088. doi:10.1038/s41467-021-21246-9 [PubMed: 33597522]
36. Qi Y, Xu Z, Zhu Q, Thomas C, Kumar R, Feng H, Dostal DE, White MF, Baker KM, Guo S. Myocardial Loss of IRS1 and IRS2 Causes Heart Failure and Is Controlled by p38α MAPK During Insulin Resistance. Diabetes. 2013;62:3887–3900. doi:10.2337/db13-0095 [PubMed: 24159000]
37. Wang Y, Christopher BA, Wilson KA, Muoio D, McGarrah RW, Brunengraber H, Zhang GF. Propionate-induced changes in cardiac metabolism, notably CoA trapping, are not altered by l-carnitine. Am J Physiol Endocrinol Metab. 2018;315:E622–E633. doi:10.1152/ajpendo.00081.2018 [PubMed: 30016154]
38. Haghikia A, Zimmermann F, Schumann P, Jasina A, Roessler J, Schmidt D, Heinze P, Kaisler J, Nageswaran V, Aigner A, et al. Propionate attenuates atherosclerosis by immune-dependent regulation of intestinal cholesterol metabolism. Eur Heart J. 2022;43:518–533. doi:10.1093/eurheartj/ehab644 [PubMed: 34597388]
39. Butte NF, Liu Y, Zakeri IF, Mohney RP, Mehta N, Voruganti VS, Göring H, Cole SA, Comuzzie AG. Global metabolomic profiling targeting childhood obesity in the Hispanic population. Am J Clin Nutr. 2015;102:256–267. doi:10.3945/ajcn.115.111872 [PubMed: 26085512]
40. Gao X, Zhang W, Wang Y, Pedram P, Cahill F, Zhai G, Randell E, Gulliver W, Sun G. Serum metabolic biomarkers distinguish metabolically healthy peripherally obese from unhealthy centrally obese individuals. Nutr Metab (Lond). 2016;13:33. doi:10.1186/s12986-016-0095-9 [PubMed: 27175209]
41. Bartolomaeus H, Balogh A, Yakoub M, Homann S, Markó L, Höges S, Tsvetkov D, Krannich A, Wundersitz S, Avery EG, et al. Short-Chain Fatty Acid Propionate Protects From Hypertensive Cardiovascular Damage. Circulation. 2019;139:1407–1421. doi:10.1161/CIRCULATIONAHA.118.036652 [PubMed: 30586752]
42. Roe ND, Handzlik MK, Li T, Tian R. The Role of Diacylglycerol Acyltransferase (DGAT) 1 and 2 in Cardiac Metabolism and Function. Sci Rep. 2018;8:4983. doi:10.1038/s41598-018-23223-7 [PubMed: 29563512]
43. Chambers KT, Cooper MA, Swearingen AR, Brookheart RT, Schweitzer GG, Weinheimer CJ, Kovacs A, Koves TR, Muoio DM, McCommis KS, et al. Myocardial Lipin 1 knockout in mice approximates cardiac effects of human LPIN1 mutations. JCI Insight. 2021;6:e134340. doi:10.1172/jci.insight.134340 [PubMed: 33986192]
44. Czibik G, Steeples V, Yavari A, Ashrafian H. Citric Acid Cycle Intermediates in Cardioprotection. Circ Cardiovasc Genet. 2014;7:711–719. doi:10.1161/CIRCGENETICS.114.000220 [PubMed: 25518044]
45. Cao J, Yuan L. Identification of key genes for hypertrophic cardiomyopathy using integrated network analysis of differential lncRNA and gene expression. Front Cardiovasc Med. 2022;9:946229. doi:10.3389/fcvm.2022.946229 [PubMed: 35990977]
46. Suffee N, Baptista E, Piquereau J, Ponnaiah M, Doisne N, Ichou F, Lhomme M, Pichard C, Galand V, Mougenot N, et al. Impacts of a high-fat diet on the metabolic profile and the phenotype

of atrial myocardium in mice. Cardiovasc Res. 2022;118:3126–3139. doi:10.1093/cvr/cvab367 [PubMed: 34971360]

47. Riemersma M, Hazebroek MR, Helderman-van den Enden ATJM, Salomons GS, Ferdinandusse S, Brouwers MCGJ, van der Ploeg L, Heymans S, Glatz JFC, van den Wijngaard A, et al. Propionic acidemia as a cause of adult-onset dilated cardiomyopathy. Eur J Hum Genet. 2017;25:1195–1201. doi:10.1038/ejhg.2017.127 [PubMed: 28853722]
48. Dai C, Li Q, May HI, Li C, Zhang G, Sharma G, Sherry AD, Malloy CR, Khemtong C, Zhang Y, et al. Lactate Dehydrogenase A Governs Cardiac Hypertrophic Growth in Response to Hemodynamic Stress. Cell Rep. 2020;32:108087. doi:10.1016/j.celrep.2020.108087 [PubMed: 32877669]
49. Park SB, Seo KW, So AY, Seo MS, Yu KR, Kang SK, Kang KS. SOX2 has a crucial role in the lineage determination and proliferation of mesenchymal stem cells through Dickkopf-1 and c-MYC. Cell Death Differ. 2012;19:534–545. doi:10.1038/cdd.2011.137 [PubMed: 22015605]
50. Koyanagi M, Iwasaki M, Rupp S, Tedesco FS, Yoon CH, Boeckel JN, Trauth J, Schütz C, Ohtani K, Goetz R, et al. Sox2 transduction enhances cardiovascular repair capacity of blood-derived mesoangioblasts. Circ Res. 2010;106:1290–1302. doi:10.1161/CIRCRESAHA.109.206045 [PubMed: 20185800]
51. Gusterson RJ, Jazrawi E, Adcock IM, Latchman DS. The Transcriptional Co-activators CREB-binding Protein (CBP) and p300 Play a Critical Role in Cardiac Hypertrophy That Is Dependent on Their Histone Acetyltransferase Activity. J Biol Chem. 2003;278:6838–6847. doi:10.1074/jbc.M211762200 [PubMed: 12477714]
52. you Zhang Y, Li X, wen Qian S, Guo L, yan Huang H, He Q, Liu Y, gu Ma C, Tang QQ. Down-regulation of type I Runx2 mediated by dexamethasone is required for 3T3-L1 adipogenesis. Mol Endocrinol. 2012;26:798–808. doi:10.1210/me.2011-1287 [PubMed: 22422618]
53. Bond ST, King EJ, Henstridge DC, Tran A, Moody SC, Yang C, Liu Y, Mellett NA, Nath AP, Inouye M, et al. Deletion of Trim28 in committed adipocytes promotes obesity but preserves glucose tolerance. Nat Commun. 2021;12:74. doi:10.1038/s41467-020-20434-3 [PubMed: 33397965]
54. Lee YS, whan Kim J, Osborne O, Oh DY, Sasik R, Schenk S, Chen A, Chung H, Murphy A, Watkins SM, et al. Increased Adipocyte O2 Consumption Triggers HIF-1α, Causing Inflammation and Insulin Resistance in Obesity. Cell. 2014;157:1339–1352. doi:10.1016/j.cell.2014.05.012 [PubMed: 24906151]
55. Antoniades C 'Dysfunctional' adipose tissue in cardiovascular disease: a reprogrammable target or an innocent bystander? Cardiovasc Res. 2017;113:997–998. doi:10.1093/cvr/cvx116 [PubMed: 28637258]
56. Berezin AE, Berezin AA, Lichtenauer M. Emerging Role of Adipocyte Dysfunction in Inducing Heart Failure Among Obese Patients With Prediabetes and Known Diabetes Mellitus. Front Cardiovasc Med. 2020;7:583175. doi:10.3389/fcvm.2020.583175 [PubMed: 33240938]
57. Schuster A, Backhaus SJ, Stiermaier T, Navarra JL, Uhlig J, Rommel KP, Koschalka A, Kowallick JT, Bigalke B, Kutty S, et al. Impact of Right Atrial Physiology on Heart Failure and Adverse Events after Myocardial Infarction. J Clin Med. 2020;9:210. doi:10.3390/jcm9010210 [PubMed: 31940959]
58. Sun H, Olson KC, Gao C, Prosdocimo DA, Zhou M, Wang Z, Jeyaraj D, Youn JY, Ren S, Liu Y, et al. Catabolic Defect of Branched-Chain Amino Acids Promotes Heart Failure. Circulation. 2016;133:2038–2049. doi:10.1161/CIRCULATIONAHA.115.020226 [PubMed: 27059949]
59. Smiseth OA, Maurer G. Focus on the left atrium in cardiac disease. Eur Heart J Cardiovasc Imaging. 2021;23:1–1. doi:10.1093/ehjci/jeab259 [PubMed: 34871359]
60. Troncoso R, Ibarra C, Vicencio JM, Jaimovich E, Lavandero S. New insights into IGF-1 signaling in the heart. Trends Endocrinol Metab. 2014;25(3):128–137. doi:10.1016/j.tem.2013.12.002 [PubMed: 24380833]
61. Abumrad NA, Goldberg IJ. CD36 actions in the heart: Lipids, calcium, inflammation, repair and more? Biochim Biophys Acta. 2016;1861:1442–1449. doi:10.1016/j.bbalip.2016.03.015 [PubMed: 27004753]

62. Shu H, Peng Y, Hang W, Nie J, Zhou N, Wang DW. The role of CD36 in cardiovascular disease. Cardiovasc Res. 2022;118:115–129. doi:10.1093/cvr/cvaa319 [PubMed: 33210138]

63. Sethi JK, Vidal-Puig A. Visfatin: the missing link between intra-abdominal obesity and diabetes? Trends Mol Med. 2005;11:344–347. doi:10.1016/j.molmed.2005.06.010 [PubMed: 16005682]

64. Pillai VB, Sundaresan NR, Kim G, Samant S, Moreno-Vinasco L, Garcia JGN, Gupta MP. Nampt secreted from cardiomyocytes promotes development of cardiac hypertrophy and adverse ventricular remodeling. Am J Physiol Heart Circ Physiol. 2013;304:H415–H426. doi:10.1152/ajpheart.00468.2012 [PubMed: 23203961]

Highlights

- Single nucleus RNA-sequencing of subcutaneous adipose and heart identified not only adipocyte marker genes shared across the two tissues but also distinct tissue-resident adipocyte marker genes.
- We discovered the propanoate metabolism pathway to be enriched among the marker genes of heart-resident adipocytes, consistently in all four heart chambers.
- Variants in the right atrium adipocyte marker genes and their *cis* regulatory regions are enriched for associations with coronary artery disease.
- Cellular communication and functional pathway analyses suggest heart chamber level coordination of heart adipocyte expression profiles, supported by the observed larger number of significant adipocyte-associated ligand-receptor interactions and functional pathways in the atriums than ventricles.

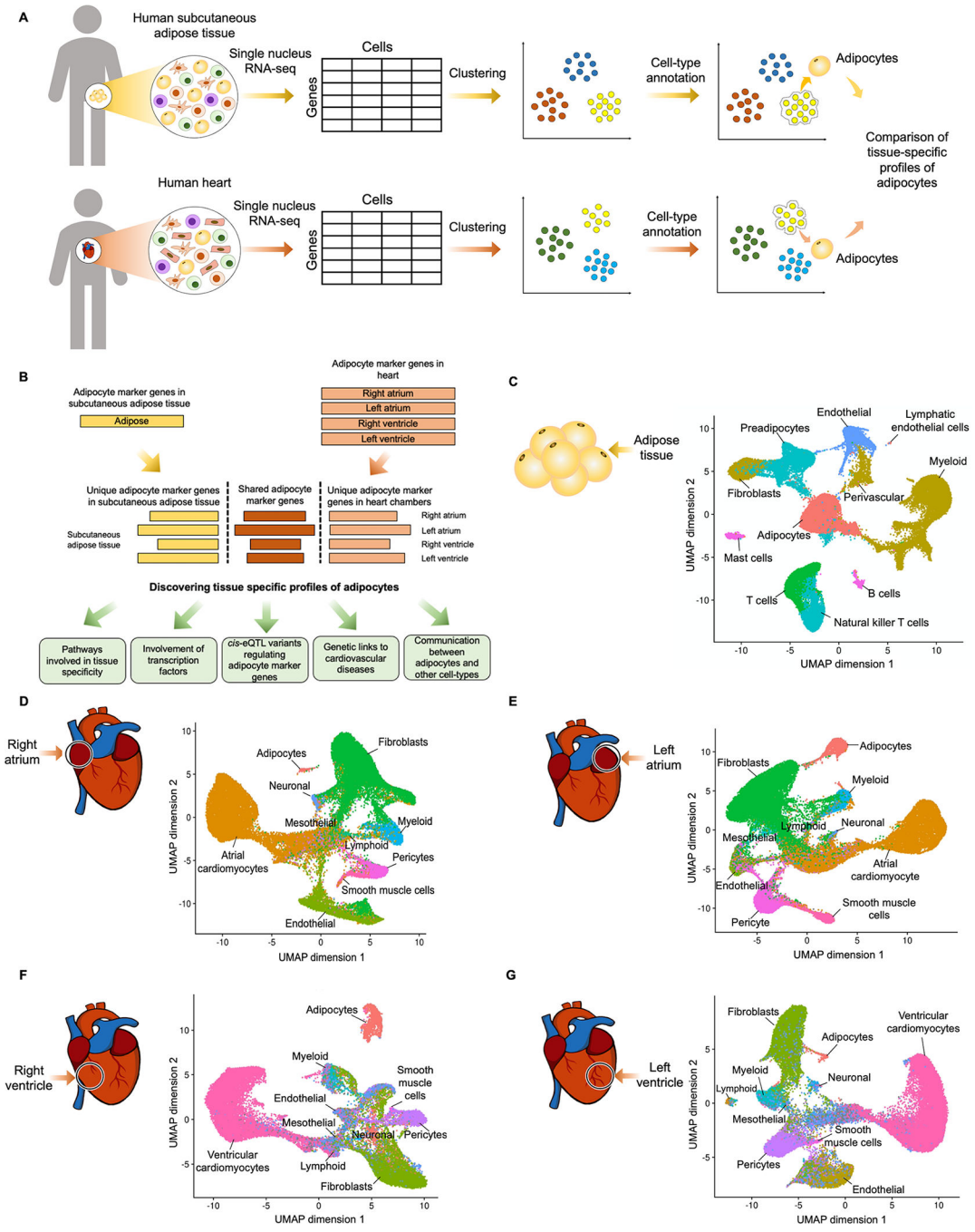

Figure 1. Cellular diversity in subcutaneous adipose tissue and each of the heart chamber.

A, Schematic overview of the single nucleus RNA-seq (snRNA-seq) analysis pipeline. Analysis of the subcutaneous adipose tissue (n=15) and heart (n=7) datasets included clustering of nuclei, followed by cell-type annotation and marker gene identification (see the Methods). **B**, Further analysis of adipocyte marker genes included identification of tissue-specific and tissue-shared adipocyte marker genes, followed by KEGG pathway enrichment analysis, transcription factor enrichment analysis, *cis*-expression quantitative trait locus (eQTL) analysis, gene set enrichment analysis for genetic disease associations,

and cell-cell communication analysis between adipocytes and other cell-types. **C**, Uniform Manifold Approximation and Projection (UMAP) clustering of 37,865 nuclei displaying cellular diversity in human subcutaneous adipose tissue. **D-G**, UMAP visualization of 41,204, 42,867, 28,696, and 39,639 nuclei of right atrium (RA), left atrium (LA), right ventricle (RV), and left ventricle (LV), respectively, displaying cellular diversity in the heart. The black circle indicates the location of each chamber in the heart.

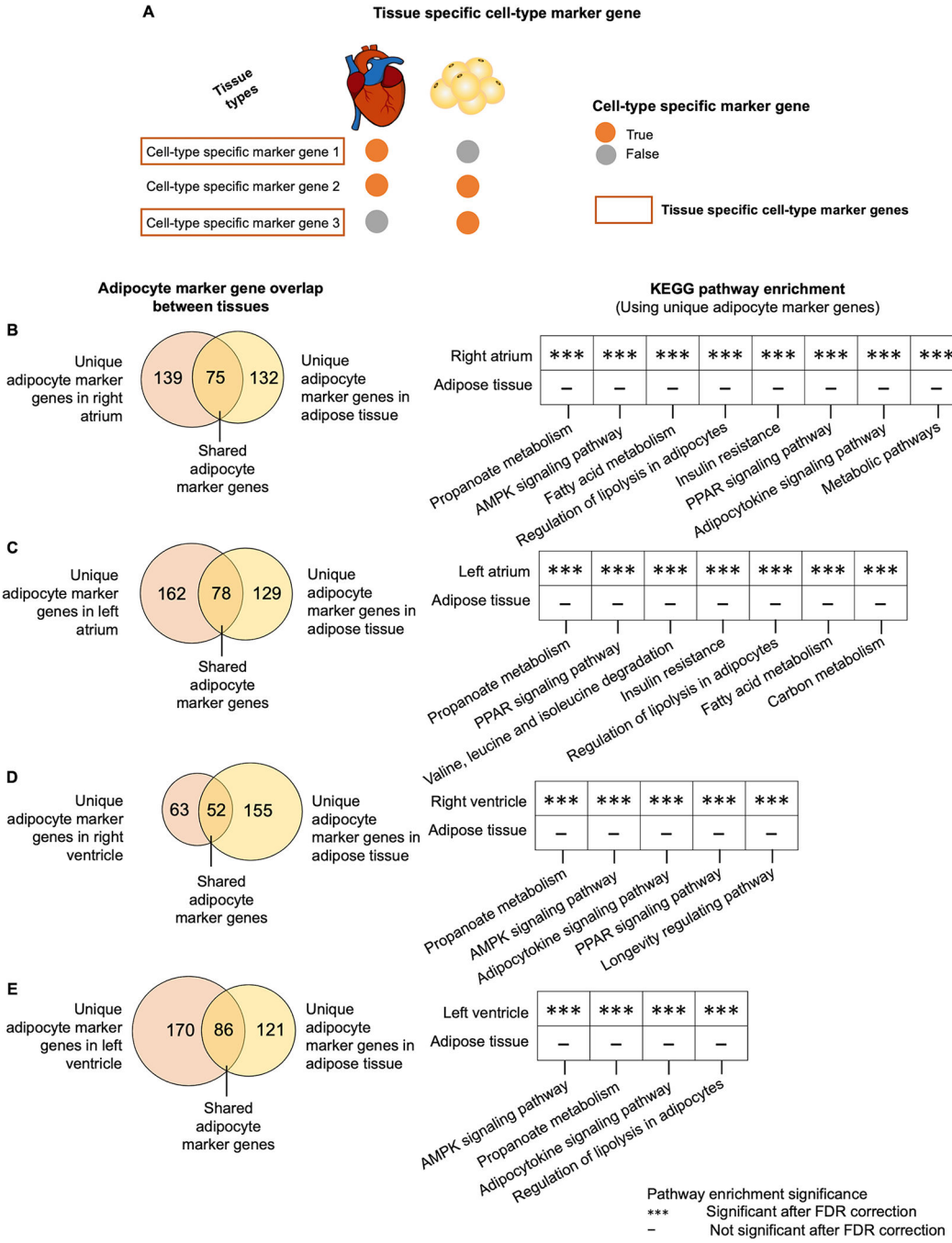

Figure 2. Comparisons of adipocyte marker genes between subcutaneous adipose tissue and heart reveal shared and tissue-specific drivers of tissue-resident adipocytes.

A, Adipocyte marker genes that are specifically present in one of the heart chambers and absent in the subcutaneous adipose tissue, and vice versa, are considered tissue-specific adipocyte marker genes. **B-E**, Overlaps of adipocyte marker genes (left) between each of the heart chambers (right atrium (RA), left atrium (LA), right ventricle (RV), and left ventricle (LV)) and subcutaneous adipose tissue; and comparison of enriched pathways using unique adipocyte marker genes (right). *P* value is calculated using hypergeometric test and adjusted

for multiple testing using BH method (FDR<0.05) (see Table S1–S5 for adipocyte marker gene lists in the subcutaneous adipose tissue, RA, LA, RV, and LV).

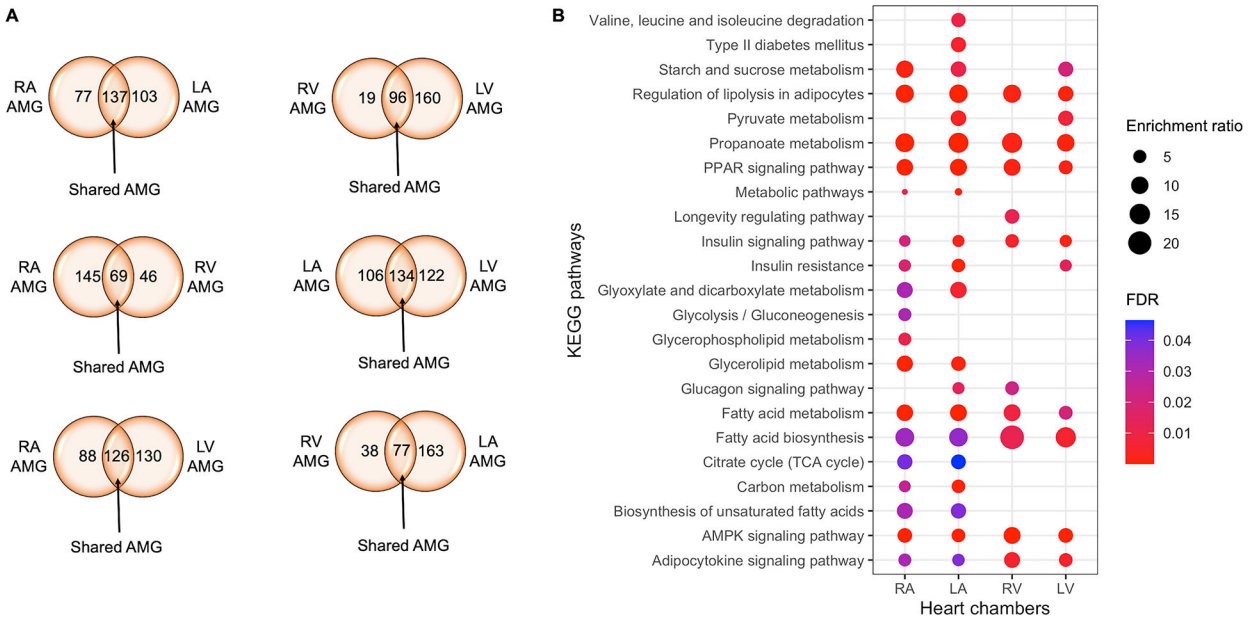

Figure 3. Comparisons of adipocyte marker genes and functional pathways between the heart chambers reveal shared and chamber-specific features of heart adipocytes.

A, Venn diagrams showing the number of shared and chamber-specific adipocyte marker genes (AMGs) between the heart chambers (right atrium (RA), left atrium (LA), right ventricle (RV), and left ventricle (LV)). **B**, Dot plot showing enriched pathways in each heart chamber (RA, LA, RV, and LV) using all adipocyte marker genes. *P* value is calculated using the hypergeometric test and adjusted for multiple testing using the BH method (FDR<0.05).

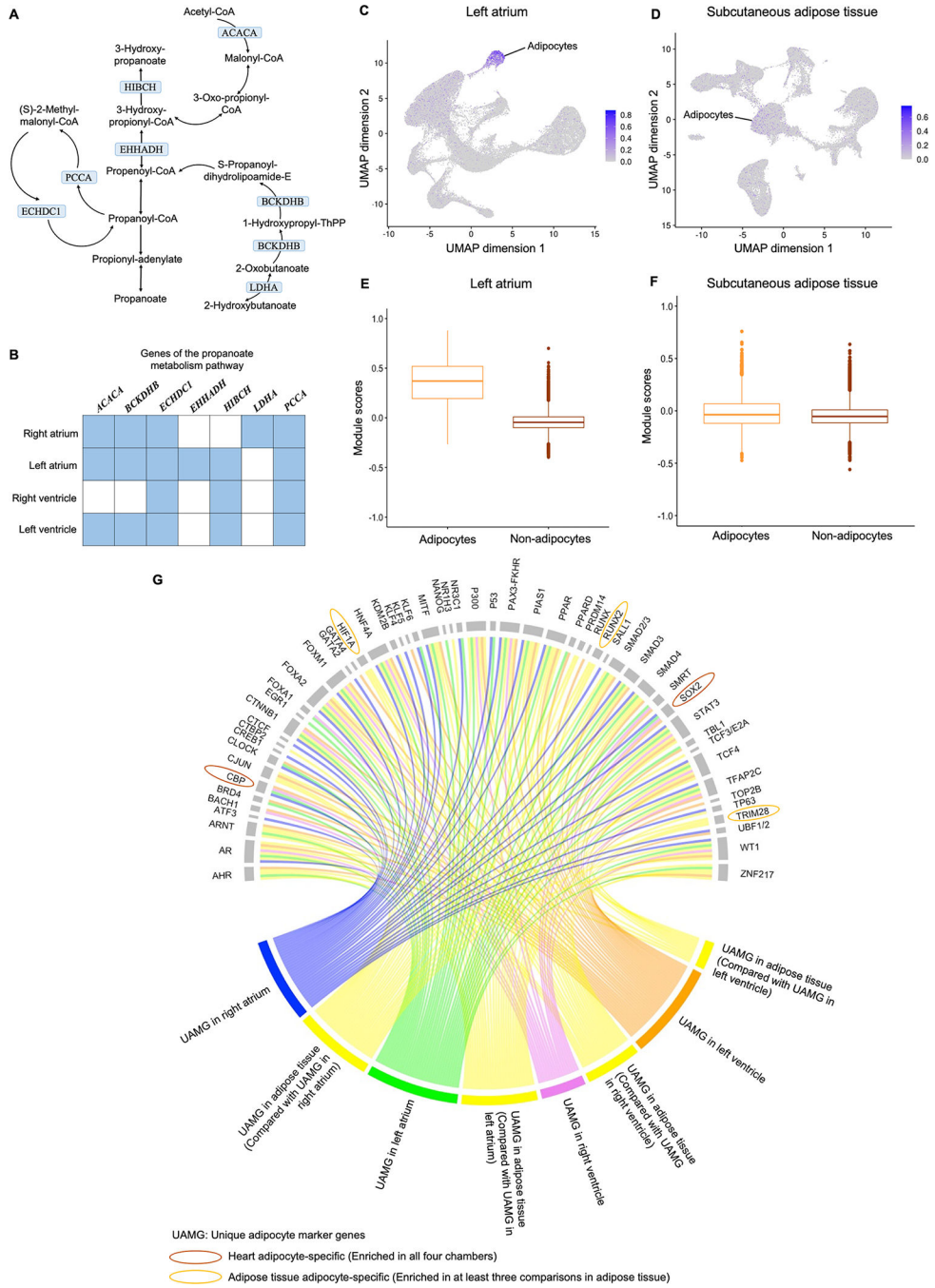

Figure 4. Module score and transcription factor (TF) enrichment analyses highlight the regulators of tissue-resident adipocytes.

Module scores analysis calculates the difference between the average expression level of genes within the module compared to aggregated expression of control gene sets. **A**, A schematic of the propanoate metabolism pathway with heart-specific adipocyte marker genes indicated by blue rectangles. **B**, Genes of the propanoate metabolism pathway among the tissue-specific adipocyte marker genes in the right atrium (RA), left atrium (LA), right ventricle (RV), and left ventricle (LV). **C**, Expression of propanoate metabolism pathway

genes is enriched in the adipocyte cluster of LA using a module score analysis (see the Methods). **D**, Expression of propanoate metabolism pathway genes is less enriched in the adipocyte cluster of the subcutaneous adipose tissue using a module score analysis. **E-F**, Box plot of module score values by cell-types (adipocytes versus non-adipocytes) in LA (E) and subcutaneous adipose tissue (F). Each box extends from the 25^{th} to the 75^{th} percentile of the distribution of the module score values in every group. The horizontal line within each box denotes the median value. In the LA, the module scores of propanoate metabolism pathway genes are significantly higher (Wilcoxon rank sum $p<2.2\times10^{-308}$; a permutation p-value=1.00×10^{-6}) in the adipocytes than non-adipocytes (Figure 4E), while in the subcutaneous adipose tissue the difference between the module scores in the adipocytes and non-adipocytes was smaller and did not pass the significance in the permutation analysis (Wilcoxon rank sum $p=9.90\times10^{-38}$; permutation p-value=0.1272) (Figure 4F). **G**, TF enrichment analysis of the unique adipocyte marker genes (UAMG) in RA, LA, RV, LV, and subcutaneous adipose tissue identifies significantly enriched TFs using the Enrichr tool[29]. Orange circle indicates heart adipocyte-specific TFs, which are enriched for all heart chambers. Yellow circle indicates adipose tissue adipocyte-specific TFs, which are enriched in at least three comparisons between subcutaneous adipose tissue and various heart chambers.

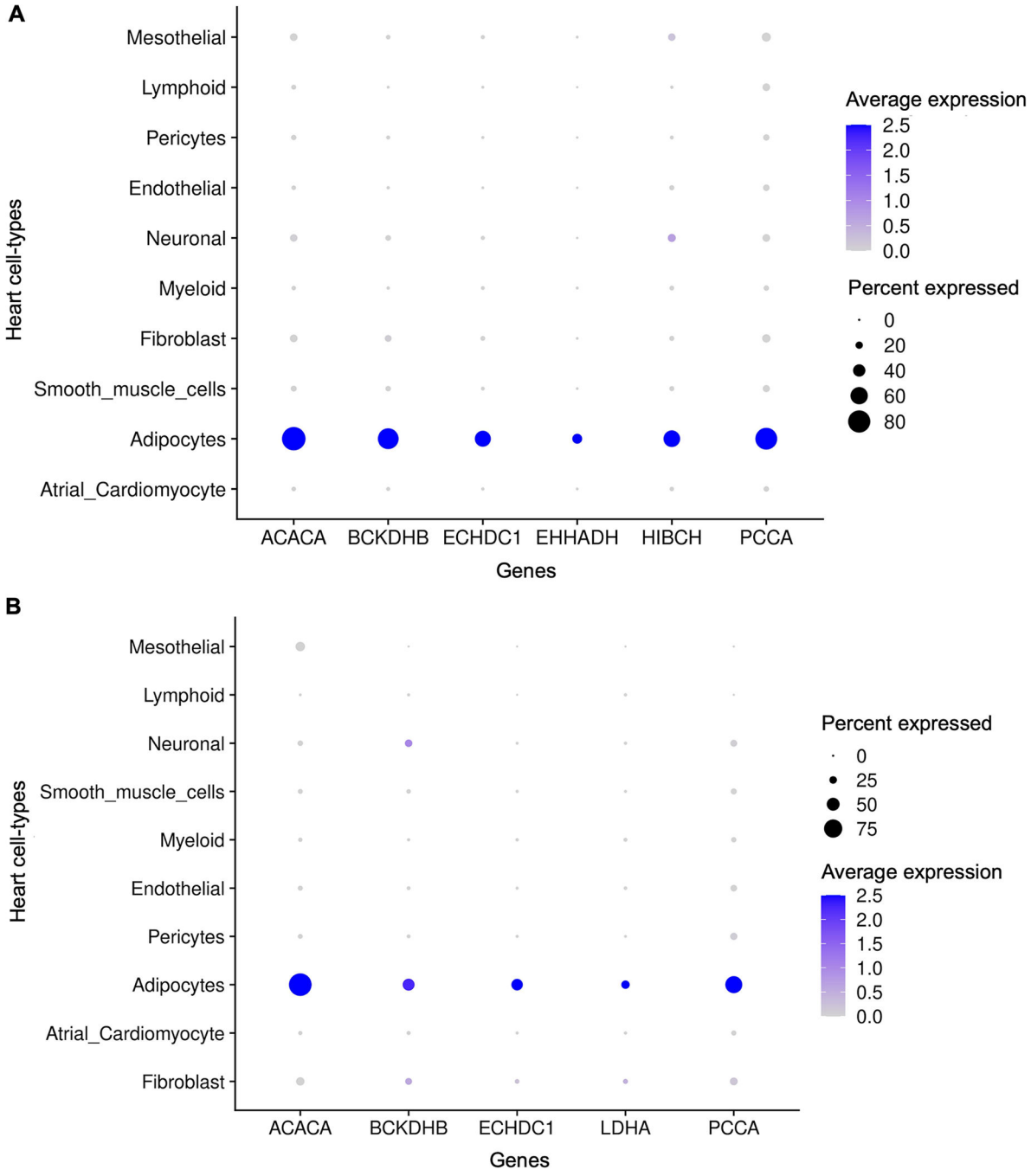

Figure 5. Comparison of mean gene expression across the cell-types reveal adipocyte-specific expression of the propanoate metabolism pathway genes in the left (A) and right atrium (B) while including all available atrium samples[6].

The dot plots of the seven propanoate metabolism pathway genes (*ACACA, BCKDHB, ECHDC1, EHHADH, HIBCH, LDHA,* and *PCCA*) show their expression profiles across the cell-types in the left atrium (n=6 samples with the mean number of adipocytes=254 nuclei/sample (SD=189)) (A) and right atrium (n=5 samples with the mean number of adipocytes=48 nuclei/sample (SD=35)) (B). The size of the dot represents the percentage of

cells where a gene is expressed within a cell-type while the color (blue is high) represents the average expression of each gene across all cells within a cell-type.

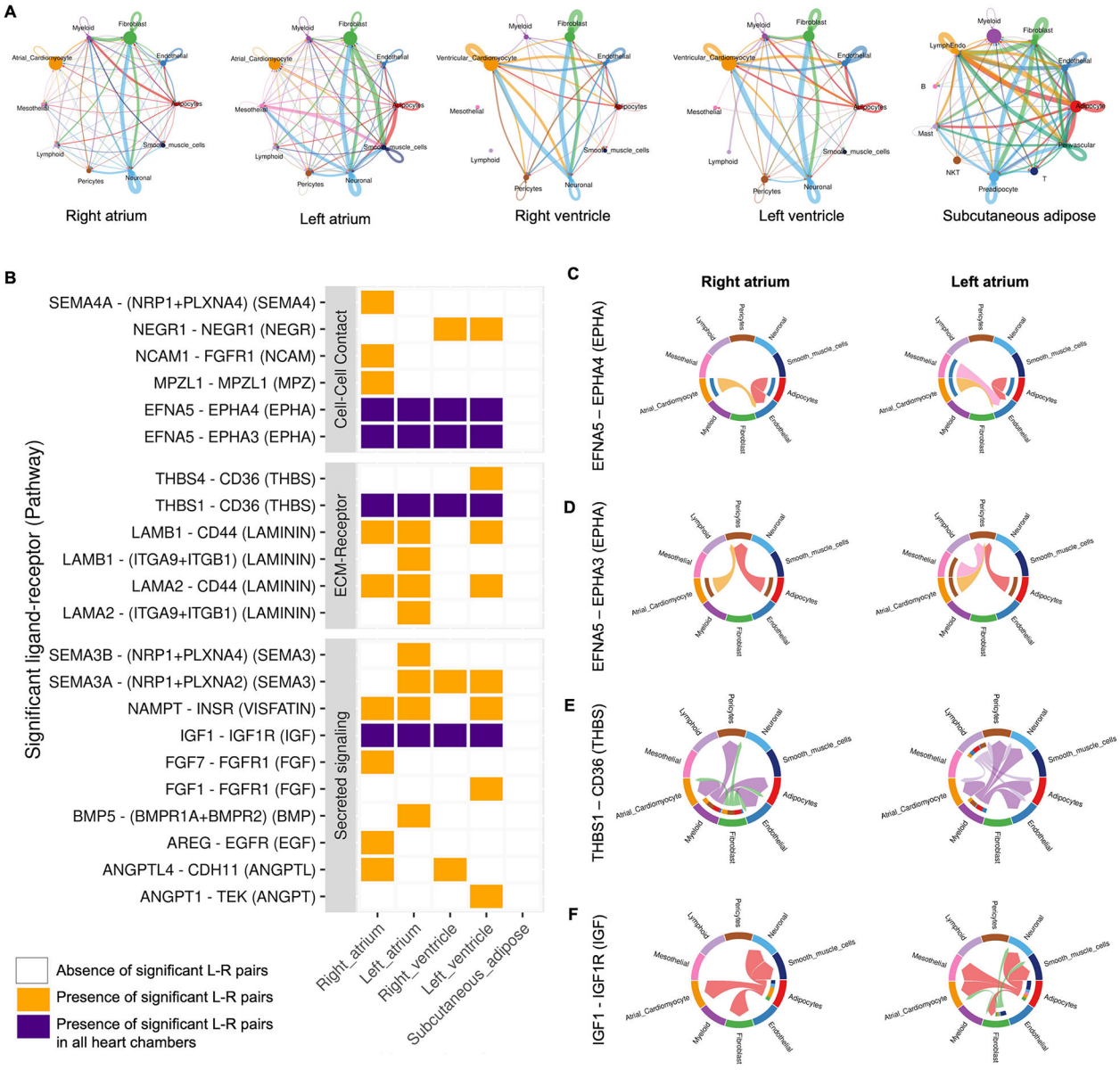

Figure 6. Cell-cell interaction analysis discovers significant heart-specific ligand-receptor interactions and signaling pathways where adipocytes represent either the sender or receiver cell-type.

. A, Circle plots showing the significant aggregated cell-cell communication networks among the cell-types in the right atrium (RA), left atrium (LA), right ventricle (RV), left ventricle (LV), and subcutaneous adipose tissue. The significant interactions (p<0.05) between two cell-types are identified using a one-sided permutation test. Lines in the circle plot indicate a significant cellular communication among the cell types, and the thickness of the lines corresponds to the relative intensity of intercellular communication. Each line is colored by the sender cell type. Plots show the strength of the interactions. Regarding the number of interactions, there are 59 adipocyte-associated ligand-receptors interactions in RA, 81 in LA, 18 in RV, and 31 in LV, respectively. **B,** Heatmap showing the presence (orange) of significant adipocyte-associated ligand-receptor (L-R) interactions in RA, LA,

RV, LV, which are absent in the subcutaneous adipose tissue. Significant L-R pairs present in all heart chambers are further highlighted in violet color. Signaling pathways associated with these L-R interactions are shown in parenthesis. Tissue-specific adipocyte-associated L-R interactions, and their corresponding probability values, *p*-values, and signaling pathways are shown in detail in Table S11–S14. **C-F**, The adipocyte-associated significant L-R pairs that were specifically present in the four heart chambers were selected for further communication analysis mediated by each L-R pair: EFNA5-EPHA4 (C), EFNA5-EPHA3 (D), THBS1-CD36 (E), and IGF1-IGF1R (F). For each L-R pair, two chord diagrams are shown indicating the sender and receiver cell-types involved in RA and LA, respectively. Chords are colored by the sender cell-type. Signaling pathways associated with these L-R interactions are given in parenthesis.

Table 1.

Coronary artery disease (CAD) GWAS variants are significantly enriched within the right atrium adipocyte marker gene regions.

Unique adipocyte marker genes	Coronary artery disease, *p*-value	Heart failure, *p*-value
Left atrium adipocyte marker genes (P_{LA}^{GSEA})	ns	0.0325
Right atrium adipocyte marker genes (P_{RA}^{GSEA})	0.0005 *	0.0312
Left ventricle adipocyte marker genes (P_{LV}^{GSEA})	ns	ns
Right ventricle adipocyte marker genes (P_{RV}^{GSEA})	ns	ns

P_{gs}^{GSEA} is the nominal gene set enrichment *p*-value for the enrichment of local variants within the particular heart adipocyte marker gene region (i.e., LA, RA, LV, RV), calculated for coronary artery disease (CAD) and heart failure (HF) GWAS summary statistics separately using the MAGENTA tool[33]. The enrichment cutoff calculated for each disease is the 95th percentile of all gene *p*-values calculated from the corresponding GWAS meta-analysis.

*Significant enrichment after Bonferroni correction ($p<0.0062$; 4 gene sets and 2 traits). ns indicates non-significant (an unadjusted $p>0.05$).